EDMS NO.	REV.	VALIDITY
1760496	**1.0**	**VALID**

REFERENCE :

REPORT

[DQ]

QUENCH PROTECTION STUDIES FOR THE HIGH LUMINOSITY LHC INNER TRIPLET CIRCUIT

Abstract

This document describes the results of the quench protection studies for the High-Luminosity LHC inner triplet circuit. The studies include a comparison between the performance of different protection system configurations, sensitivity analyses to conductor parameters, and failure scenarios.

TRACEABILITY

Prepared by: E. Ravaioli (Lawrence Berkeley National Laboratory, Berkeley, CA)	***Date:*** 2016-11-04
Verified by: F. Menendez Camara, F. Rodriguez Mateos, GL. Sabbi (Lawrence Berkeley National Laboratory, Berkeley, CA), H. Thiesen, A. Verweij, S. Yammine	***Date:*** 2017-03-16
Approved by: G. Ambrosio (Fermilab National Laboratory, Batavia, IL), A. Ballarino, I. Bejar Alonso, J.-P. Burnet, R. Denz, P. Ferracin, E. Todesco, D. Wollmann	***Date:*** 2017-04-19
Distribution: N. Surname (DEP/GRP) *(in alphabetical order) can also include reference to committees*	

Rev. No.	***Date***	***Description of Changes*** *(major changes only, minor changes in EDMS)*

Table of contents

1 INTRODUCTION

Various options for the quench protection of the HL-LHC inner triplet circuit are under study, including quench heaters (QH) glued to the outer (O-QH) and inner (I-QH) layers of the coils and Coupling-Loss Induced Quench (CLIQ) [1] units electrically connected to the coils.

The choice of the protection system has an impact on the temperature reached in the coil's hot-spot at the end of the discharge, on the peak voltages to ground and between coil sections developed during the transient, and on the peak stresses reached in the conductor.

2 HL-LHC INNER TRIPLET CIRCUIT

The current baseline for the circuit includes six magnets powered by one main power supply and three trim power supplies [2]. An energy extraction is not part of the circuit, since several analyses showed that its installation in this circuit is not efficient from a protection point of view [3-5]. Each supply is by-passed by a crowbar including back to back thyristors. An additional string of diodes is included in the circuit to allow the flowing of different currents in Q2a and Q2b during the discharge and to limit the voltage to ground. This unbalance in the currents flowing in the magnets at the moment of the quench can be due to: non zero currents provided by the trim supplies; different currents introduced by the CLIQ units connected to different magnets; slightly different strand/cable parameters in the coils, which results in a different discharge velocity.

The following figure shows the electrical scheme of the circuit, including all quench protection elements under consideration (O-QH, I-QH, CLIQ).

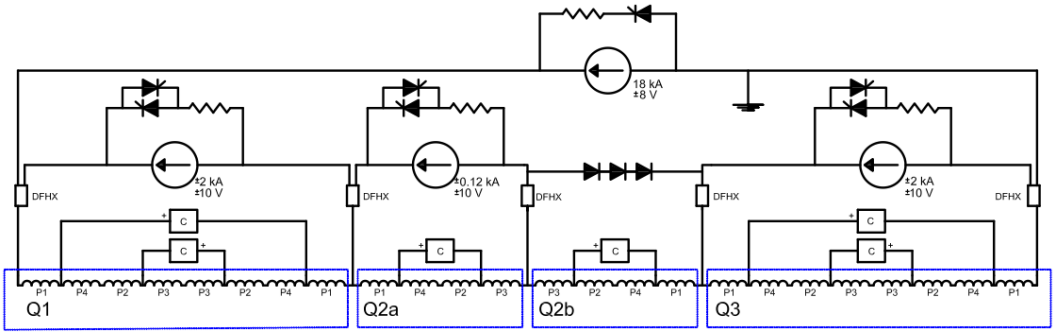

Figure 1. Electrical scheme of the HL-LHC inner triplet circuit.

3 REFERENCE MAGNET, CABLE AND STRAND PARAMETERS

The following tables summarize the main parameters used in the simulations presented in this document and the ranges considered for their variation [6-7]. When not otherwise stated in the text, these are the parameters assumed in the analysis. Note the use of cable/strand dimensions after reaction.

Table 1. Main magnet parameters used in the simulations [6-7]

Parameter	Unit	Q1/Q3	Q2a/Q2b
Nominal current, I_{nom}	A	16471	
Peak field in the conductor at I_{nom}	T	11.4	
Ultimate current, I_{ult} A	A	17800	
Operating temperature	K	1.9	
Magnetic length	m	2x4.20	7.15
Differential inductance at I_{nom}	mH	2x34.4	58.6
Stored energy at I_{nom}	MJ	2x4.7	7.9
Number of turns per pole	-	50	

Note: Each "magnet" is defined in this document as a unit of the magnetic length specified in this table

Table 2. Main conductor and insulation parameters used in the simulations [6-7]

Parameter	Unit	Value	Range
Superconductor composition	-	Ti-alloyed Nb3Sn	
Number of strands	-	40	
Strand diameter	mm	0.85	±0.003
Bare cable width	mm	18.363	
Bare cable thickness	mm	1.594	
Cable insulation thickness	mm	0.145	
Inter layer insulation thickness	mm	0.660	
Copper/non-Copper ratio	-	1.15	1.1-1.3
Filament twist pitch	mm	19	
Strand twist pitch	mm	109	
RRR of the copper matrix	-	200	100-350
Effective transverse resistivity of the strand matrix	-	0.75	0.5-2
Cross-contact resistance between strands	μΩ	10	0.1-100

4 REFERENCE QUENCH PROTECTION SYSTEM PARAMETERS

Three quench protection elements, and combinations of those, are considered

- QH attached to the outer layers of the coils (O-QH)
- QH attached to the inner layers of the coils (I-QH)
- Coupling-Loss Induced Quench (CLIQ) units electrically connected to the coils.

The following tables summarize the main parameters used in the simulations presented in this document. As a current assumption, QH strips are powered by standard LHC power supplies, whereas the parameters of the CLIQ units can still be optimized. The design of the quench-heater strips follows the "Copper-plated heater design 2 (IL/OL)" proposed in [6].

Table 3. Main O-QH parameters used in the simulations

Parameters	Unit	Q1/Q3	Q2a/Q2b
Number of QH supplies per magnet*	-	8	8
QH supply charging voltage	V	600**	900
QH supply capacitance	mF	7.05	7.05
QH supply voltage to ground	V	±300**	±450
Number of QH strips connected in series	-	2	2
Thickness of the kapton insulation between strip and coil	µm	50	50
Resistance of each QH strip at T=10 K	Ω	1.14	1.98
Warm resistance of the QH leads	Ω	0.6	0.6
Peak power density	W/cm^2	236	213
Discharge time-constant	ms	20	32
Triggering time	ms	5***	

*Each "magnet" is defined in this document as a unit of the magnetic length specified in Table 2

**Standard LHC QH power supplies need to be modified to provide this charging voltage. Alternatively, a room temperature resistance could be added to the QH discharge circuit.

***Standard LHC QH power supplies may be modified to provide a faster triggering time (target: 1 ms), but conservatively the present value of 5 ms is used

Table 4. Main I-QH parameters used in simulations

Parameters	Unit	Q1/Q3	Q2a/Q2b
Number of QH supplies per magnet*	-	4	4
QH supply charging voltage	V	600**	900
QH supply capacitance	mF	7.05	7.05
QH supply voltage to ground	V	±300**	±450
Number of QH strips connected in series	-	2	2
Thickness of the kapton insulation between strip and coil	µm	50	50
Resistance of each QH strip at T=10 K	Ω	1.81	3.06
Warm resistance of the QH leads	Ω	0.6	0.6
Peak power density	W/cm2	110	98
Discharge time-constant	ms	30	47
Triggering time	ms	5***	

*Each "magnet" is defined in this document as a unit of the magnetic length specified in Table 2

**Standard LHC QH power supplies need to be modified to provide this charging voltage. Alternatively, a room temperature resistance could be added to the QH discharge circuit.

***Standard LHC QH power supplies may be modified to provide a faster triggering time (target: 1 ms), but conservatively the present value of 5 ms is used

Table 5. Main CLIQ parameters used in the simulations

Parameters	Unit	Q1/Q3	Q2a/Q2b
Number of CLIQ units per magnet	-	1**	1
CLIQ charging voltage	V	600	1000
Capacitance of the CLIQ capacitor bank	mF	40***	40***
Induced voltage to ground at the triggering	V	±300	±500
Resistance of the CLIQ discharge circuit	Ω	0.05***	
Triggering time	ms	1	

*Each "magnet" is defined in this document as a unit of the magnetic length specified in Table 2

** In the Q1/Q3 magnets, two CLIQ units are connected to two magnets (see Figure 1)

***The values of CLIQ capacitance and circuit resistance may be partially reviewed after the MQXFS1b test campaign, see following sections

5 OPTIONS FOR THE QUENCH PROTECTION SYSTEM

The choice of the protection system has an impact on the temperature reached in the coil's hot-spot at the end of the discharge, on the peak voltages to ground and between coil sections developed during the transient, and on the peak stresses reached in the conductor. Three quench protection options are analysed:

- O-QH only
- O-QH and I-QH
- O-QH and CLIQ.

5.1 Circuit modelling

The discharge of the circuit after a quench in one of the six magnets is simulated using the TALES (Transient Analysis with Lumped-Elements of Superconductors) application [8], which includes inter filament and inter strand coupling loss, quench back and reduction of the differential inductance due to dynamic effects. This software allows simultaneously modelling the electrodynamics of the circuit, including power supplies, magnets, parallel elements, busbars, and the electro-thermal transient in the magnet (2D model).

There are many possible combinations of initial currents in the main and three trim power supplies. In this document, two examples are presented to illustrate the dynamics of the currents in all branches of the circuit:

- Case A: Magnets are protected by CLIQ and O-QH. Nominal current in the main power supply, zero currents in all trim power supplies (I_{MS}=16.5 kA, I_{TS1}=I_{TS2}=I_{TS3}=0);
- Case B: Magnets are protected by CLIQ and O-QH. Nominal current in the main power supply, nominal currents in all trim power supplies (I_{MS}=16.5 kA, I_{TS1}=I_{TS3}=-2.0 kA, and I_{TS2}=-0.12 kA).

The simulated currents through the magnet sections, parallel diodes, and current leads for the above mentioned Case A are shown in Figures 2a-2b. At t=0, the power supplies are switched off and the O-QH and CLIQ units are triggered. A current of less than 1 kA is introduced through the diode D3 just after triggering CLIQ.

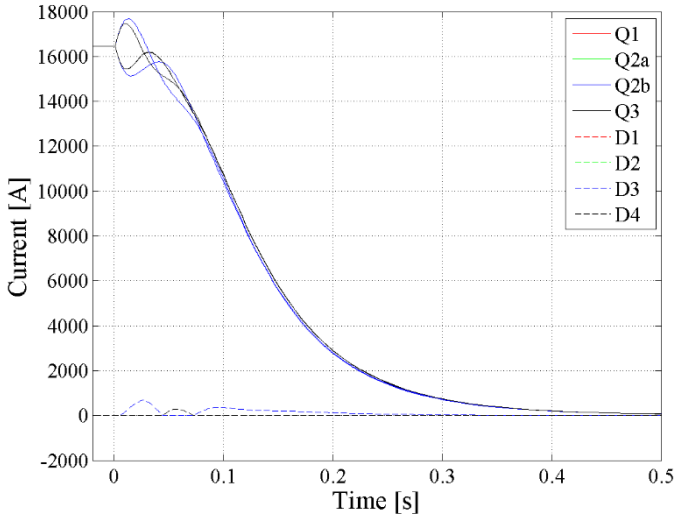

(a)

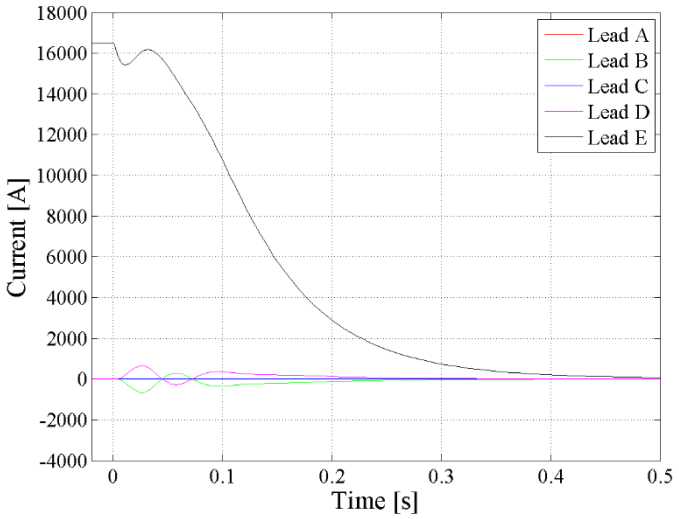

(b)

Figure 2. Simulated currents in the magnets and parallel diodes (a) and in the current leads (b) after a quench at nominal current, with zero current in all trim power supplies.

The simulated currents for Case B are shown in Figures 3a-3b. Current leads LB and LD carry the unbalanced currents between Q1-Q2a and Q2b-Q3, respectively. The magnets with higher initial current are discharged more quickly due to the higher resistances developed in their coils during the quench induced by the protection system. Hence, the currents through LB and LD invert their polarities during the discharge. Lead LC carries the current unbalance between Q2a-Q2b, which is relatively small throughout the transient.

The peak currents and current changes in each of the five current leads, calculated for Cases A and B, are reported in Tables 6 and 7. The implementation of CLIQ increases the peak currents in the leads only by a few hundred A. On the contrary, the peak current changes roughly double due to the high current changes imposed by CLIQ just after triggering.

Other cases are interested to study, including a beam-induced quench in one magnet, which may turn large parts of the coil (in the worst case, the entire coil) to the normal state. Additional simulations are under way. Preliminary results show peak currents of up to 5 kA in Leads B and D, and up to 3 kA in Lead C.

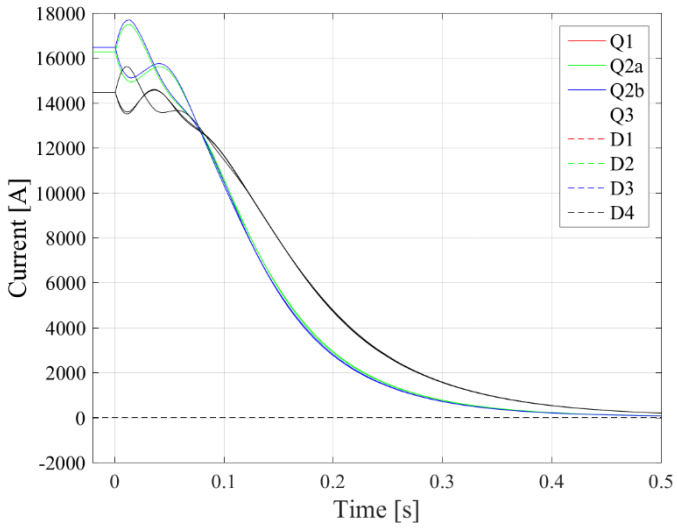

(a)

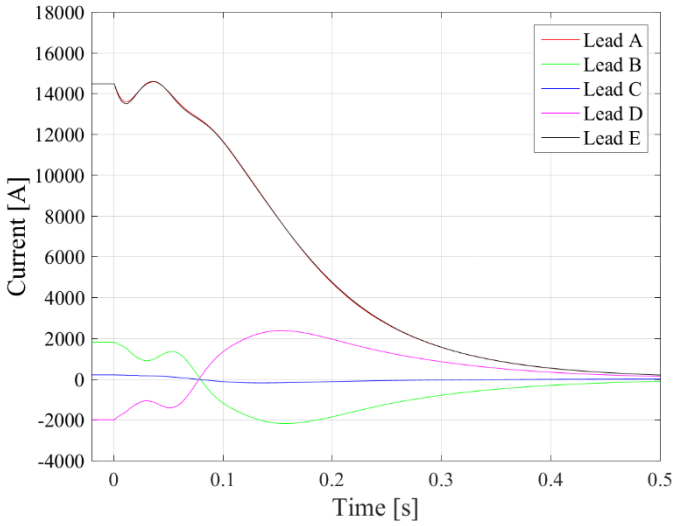

(b)

Figure 3. Simulated currents in the magnets and parallel diodes (a) and in the current leads (b) after a quench at nominal current, with maximum currents in all trim power supplies.

Table 6. Simulated peak currents in the circuit current leads (see Figure 1) after a quench at nominal current, in units of kA

Configuration	Lead A	Lead B	Lead C	Lead D	Lead E
Case A – Zero current in trim power supplies					
O-QH	16.5	0.1	0	0.1	16.5
O-QH + I-QH	16.5	0	0	0	16.5
O-QH + CLIQ	16.5	0.8	0	0.8	16.5
Case B – Nominal current in trim power supplies					
O-QH	14.5	2.0	0.1	2.2	14.5
O-QH + I-QH	14.5	1.8	0.1	2.0	14.5
O-QH + CLIQ	14.6	2.2	0.1	2.4	14.6

Table 7. Simulated peak current rate changes in the circuit current leads (see Figure 1) after a quench at nominal current, in units of kA/s

Configuration	Lead A	Lead B	Lead C	Lead D	Lead E
Case A – Zero current in trim power supplies					
O-QH	106	9	3	9	106
O-QH + I-QH	111	9	0	9	111
O-QH + CLIQ	174	55	4	55	195
Case B – Nominal current in trim power supplies					
O-QH	74	48	10	53	74
O-QH + I-QH	76	42	9	47	76
O-QH + CLIQ	170	77	19	80	192

5.2 Electro-magnetic and thermal modelling

The presence of parallel elements across each cold mass (thyristors, diodes), limiting the voltage across it to a few volt, allows simulating the discharge of each magnet separately with good approximation. The case of the 7 m long magnet is more challenging from a protection standpoint, and is thus analysed in greater detail. The discharge of one of the six magnets is simulated using the LEDET (Lumped Element Dynamic Electro-Thermal) application [9], which includes inter filament and inter strand coupling loss, quench back and reduction of the differential inductance due to dynamic effects. With respect to TALES, this code is less flexible (only simulates single magnet circuits) but runs about 10 times faster and provides a more precise approximation of the coupling loss developed in the superconductor and of the voltages to ground internal to the magnet.

The model adopted for the magnet is 2D and assumes homogeneous temperature within each turn. The hot-spot temperature is calculated adiabatically assuming a quench starting 15 ms before the quench detection and validation. For each case, two different conditions are simulated:

- Temperature of the half of the turn where the hot-spot is located does not increase before the quench protection system is triggered. This approach usually leads to a conservative estimation of the hot-spot temperature, but to a non conservative estimation of the peak voltages.
- Half of the turn where the hot-spot is located is switched to the normal state when the quench starts. This approach usually leads to a conservative estimation of the peak voltages, but to a non conservative estimation of the hot-spot temperature. For each case, eight different possible locations for the quench start are considered, in the highest field turn of each layer (each of the four pole has two layers).

The model could be improved by simulating the actual temperature, voltage, and resistance increase in the initial hot-spot, including quench propagation in the direction of the transport current.

The simulated hot-spot temperature T_{hot} [K], peak voltage to ground $U_{g,peak}$ [V], and peak turn to turn voltage $U_{t,peak}$ [V], after a quench at nominal (I_{nom}=16.5 kA) and ultimate current (I_{ult}=17.8 kA), for the three considered protection options, are reported in Table 8. This set of simulations assumes uniform cable/strand parameters in the four poles of each magnet, which is not a conservative assumption. The uncertainty ranges in the simulated values are due to the different considered quench locations. For a graphical representation of these results, see Figures 4a, 4b and 4c in the next chapter, which also include the effect of a variation of the strand parameters.

In the case of a quench protection system based only on O-QH, the hot spot temperature after a quench at nominal current is slightly below 350 K, which is considered the safe temperature limit with respect to permanent degradation (see Figure 4a) [10]. At ultimate current, this limit is overcome and the simulated hot spot temperature approaches the physical limit of 385 K, at which permanent damage of the insulation material is expected. Furthermore, as explained in the next section, in this case the dependence of the hot spot temperature on the strand parameters is significant. The peak voltage to ground and turn to turn voltage vary significantly with the position of the quench origin; quenches starting in the inner layer and/or in the two poles to which the leads are connected result in higher Ug,peak.

The implementation of I-QH or CLIQ, together with O-QH, reduces the hot spot temperature by 80 100 K at nominal and ultimate current. Either system can maintain the T_{hot} well below 300 K at ultimate current. Also, the peak turn to turn voltage is reduced by about 30% with respect to the O-QH case. On the contrary, the peak voltage to ground is increased by about 70 V and 150 V by implementing I-QH or CLIQ, respectively.

Table 8. Simulated hot spot temperature, peak voltage to ground and peak turn to turn voltage obtained after a quench at nominal and at ultimate current, for default conductor parameters. Uncertainty ranges are due to the different quench location

Configuration	T_{hot} [K]	$U_{g,peak}$ [V]	$U_{t,peak}$ [V]
Nominal current			
O-QH	330-345	352-577	74-113
O-QH + I-QH	251-253	490-561	54-83
O-QH + CLIQ	236-238	564-641	58-83
Ultimate current			
O-QH	352-369	408-808	86-133
O-QH + I-QH	276-279	616-725	65-101
O-QH + CLIQ	260-262	748-874	71-101

6 SENSITIVITY TO STRAND PARAMETERS

The impact of the main strand parameters on the quench protection performance is analysed. Given the high number of parameters and possible combinations of their distributions in the magnet, it is difficult to define an absolute worst case. Firstly, the effect of a uniform variation of the parameters in the entire magnet is assessed. Secondly, an example of a non uniform distribution of one parameter in one of the four poles is presented.

6.1 Strand parameters uniform in the magnet conductor

The effects of a uniform variation of the strand parameters on the quench protection performance can be assessed by observing Figures 4a-c, where the simulated hot spot temperature, peak voltage to ground and turn to turn voltage are shown for varying strand parameters, namely

- RRR variation between 100 and 300
- Fraction of copper (f_{Cu}) variation between 1.1/(1.1+1)=52.4% and 1.3/(1.3+1)=56.5%
- Strand diameter (d_s) variation between 0.847 and 0.853 mm.

The same results are reported in Table 9. Uncertainty ranges also include the effect of different quench locations. In each of these simulations, the same variation of the strand parameters is assigned to the

conductor of the entire magnet. The effect of a non uniform distribution of strand parameters in the magnet is analysed in the following section.

For all three analysed quench protection options, the minimum hot spot temperature and peak voltages are obtained for the combination RRR=100, f_{Cu}=56.5% and d_s=0.853 mm; vice versa, the maximum values are obtained for the combination RRR=300, f_{Cu}=52.4% and d_s=0.847 mm. Of the three analysed parameters, f_{Cu} is the one that affects the most the protection performance; RRR and ds slightly affect the hot spot temperature, but do not significantly affect the peak voltages.

The option O-QH has the largest uncertainty on the protection performance associated to a variation of the strand parameters. For the worst set of parameters, in this configuration T_{hot} reaches above 350 K at I_{nom} and above 385 K at I_{ult}. Furthermore, $U_{t,peak}$ is about 50% higher than in the configurations including I-QH or CLIQ, approaching 150 V at I_{ult}.

The configuration including a CLIQ unit yields higher voltages to ground with respect to the other cases, in particular at I_{ult}. The peak voltages may be partly reduced by decreasing the charging voltage and/or capacitance of the CLIQ unit. This possibility will be explored after analysing the results of the quench protection studies on the MQXFS1b magnet.

Table 9. Effect of strand parameters on quench protection performance. Simulated hot spot temperature, peak voltage to ground and peak turn to turn voltage obtained after a quench at nominal and at ultimate current, for varying fraction of copper in the conductor, RRR and strand diameter. Uncertainty ranges also include the effect of different quench locations

Configuration	T_{hot} [K]	$U_{g,peak}$ [V]	$U_{t,peak}$ [V]
Nominal current			
O-QH	293-364	304-619	62-123
O-QH + I-QH	230-263	438-592	46-90
O-QH + CLIQ	215-248	521-658	49-90
Ultimate current			
O-QH	312-389	362-860	72-145
O-QH + I-QH	253-290	552-766	57-109
O-QH + CLIQ	237-273	664-924	61-109

The effect of a variation of the effective transverse resistivity in the strand matrix (affecting inter filament coupling losses) and of the cross contact resistance between strands (affecting inter strand coupling losses) is analyzed and found negligible. For each of the three quench protection options, variations of 50% 200% of the effective transverse resistivity and of 0.1 1000 μΩ of the cross contact resistance yield a variation of but a few kelvin in the T_{hot} and of but a few volt in $U_{g,peak}$ and $U_{t,peak}$.

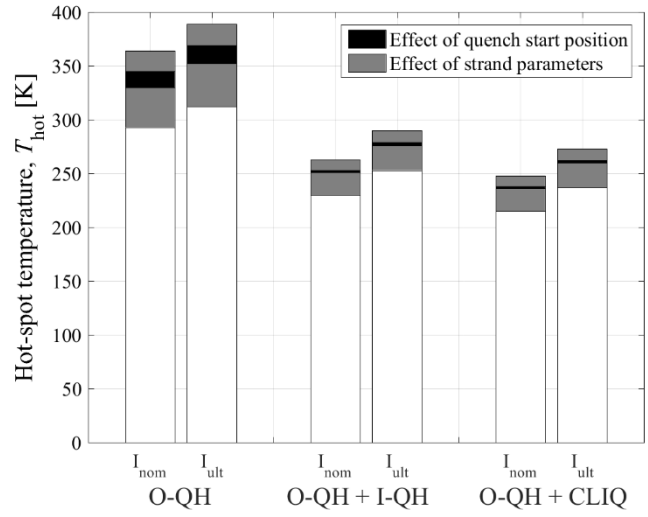

(a)

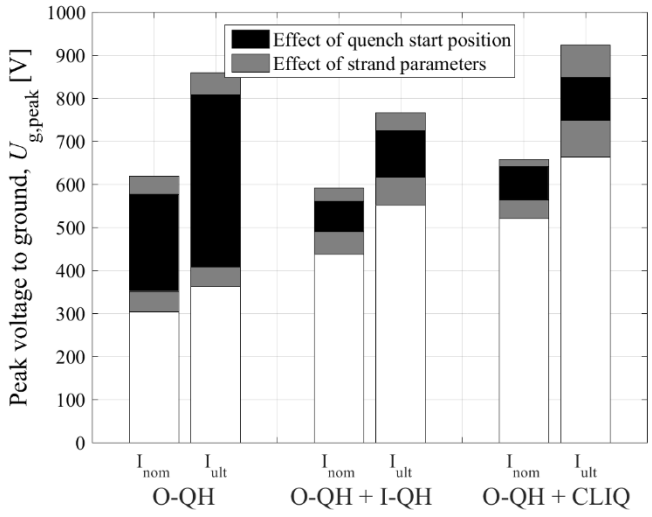

(b)

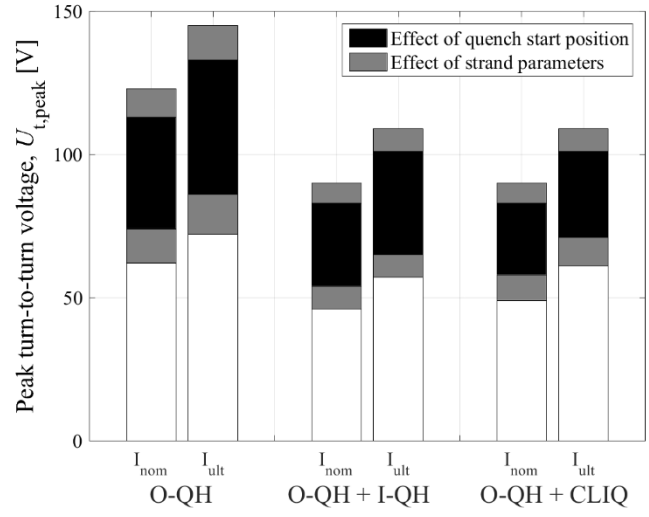

(c)

Figure 4. Effect of strand parameters on quench protection performance. Simulated hot spot temperature (a), peak voltage to ground (b) and peak turn to turn voltage (c) obtained after a quench at nominal and at ultimate current, for varying fraction of copper in the conductor, RRR and strand diameter. Uncertainty ranges also include the effect of different quench locations.

6.2 Strand parameters not uniform in the magnet conductor

A non uniform variation of the strand parameters in the magnet conductor generally results in poorer quench protection performance. In fact, in this case the parts of the magnet with lower RRR, f_{Cu} and/or ds are heated more quickly than others, whereas the parts with higher RRR, f_{Cu} and/or ds develop less resistance and hence the magnet current is discharged less quickly. Furthermore, the inhomogeneous heating of the coil results in less uniform temperature distribution in the coil cross section, and in turn less uniform voltage distribution and higher peak voltages.

It is difficult to define an absolute worst case, which should account for a high number of parameters and possible combinations of their distributions in the magnet. Here, the case of one pole characterized by one parameter significantly different from the other three poles is proposed as an example. The strand specifications state that virgin strands must have RRR≥150; however, from observation of the recent strand production, a value RRR>300 seems more likely for most of the batches of strands. It is not excluded that one or a few strand batches may have a RRR just above 150, resulting in an overall RRR of one pole of as low as 100 after cabling and winding. The assumption of uniform strand parameters in the conductor of each individual coil (pole) seems reasonable and is applied to this analysis. For these reasons, the case of one pole of the magnet characterized by a RRR significantly lower than the other three is selected to show the impact of a not uniform distribution of one strand parameter that can plausibly occur.

The electrical position of the pole with different RRR can be optimized in order to reduce the peak voltages to ground due to the non uniform distribution of voltages. If one pole has significantly lower RRR, it is better to not connect it as first or last pole (“1st”, “4th”), but in second or third position (“2nd”, “3rd”). As shown in Figures 5a 5b and in Table 10, this expedient reduces $U_{g,peak}$ by 120 250 V at I_{nom} and by 150 300 V at I_{ult}. On the contrary, the electrical position of the low RRR pole has no influence on the hot spot temperature and on the peak turn to turn voltage.

This example, although considering a rather extreme case of non uniform RRR distribution, confirms the importance of monitoring the strand parameters during the coil manufacturing process and of optimizing the order of the poles based on this information. It is strongly advised that the pole order for each produced magnet is selected based also on quench protection considerations.

In a similar way, a non uniform distribution of other strand parameters, such as the copper fraction and the strand diameter, leads to similar increases of the peak voltages to ground. It is advised to form cables composed of strands of varied f_{Cu} and ds, to minimize the possibility of winding an entire pole with values of f_{Cu} and ds close to the extremes of their ranges defined in the strand specifications.

Table 10. Effect of non uniform distribution of strand parameters on quench protection performance. Simulated peak voltage to ground obtained if one pole has RRR=150 whereas the other three have RRR=350, in the case the low RRR pole is in 1st, 2nd, 3rd or 4th electrical position. Uncertainty ranges are due to the different quench location

Configuration	T_{hot} [K]	$U_{g,peak}$ [V]				$U_{t,peak}$ [V]
		1st	2nd	3rd	4th	
Nominal current						
O-QH	350-367	514-810	411-624	412-656	478-811	85-125
O-QH + I-QH	266-268	634-734	558-658	501-546	681-778	61-92
O-QH + CLIQ	250-251	660-738	546-606	545-578	765-845	57-91
Ultimate current						
O-QH	371-390	556-945	483-828	497-744	527-1054	96-145
O-QH + I-QH	291-294	752-906	667-821	639-681	816-967	74-111
O-QH + CLIQ	260-275	850-976	705-822	686-810	987-1114	70-110

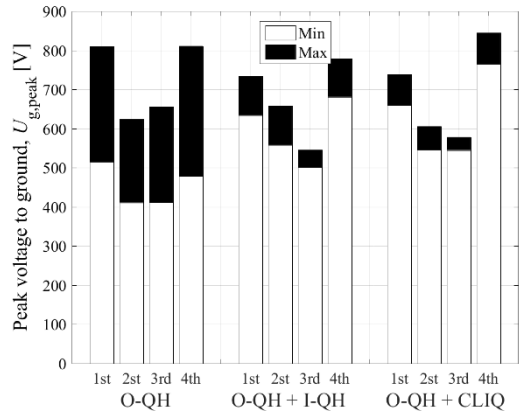

(a)

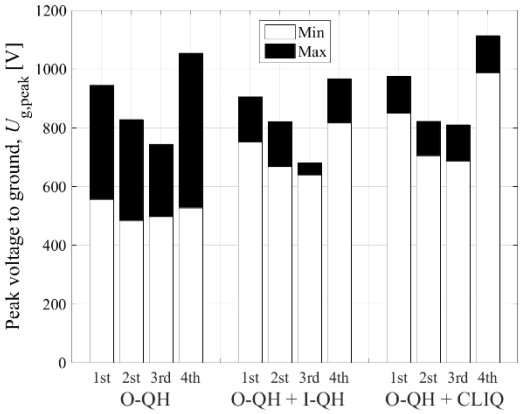

(b)

Figure 5. Effect of non-uniform distribution of strand parameters on quench protection performance. Simulated peak voltage to ground obtained if one pole has RRR=150 whereas the other three have RRR=350, in the case the low-RRR pole is in 1st, 2nd, 3rd or 4th electrical position. Uncertainty ranges are due to the different quench location. a. At nominal current. b. At ultimate current.

7 FAILURES CASES AND REDUNDANCY

The magnet quench protection is studied in the case of failure of one or more elements of its system. Both the O-QH and I-QH systems are composed of various QH power supply units and circuits, each of which is not redundant. The redundancy of the system is achieved by an increased number of QH circuits. On the contrary, the CLIQ units are designed to be operative even in the case of failure of some internal components (redundant capacitor bank, discharge system, triggering system, charging system). Thus, only the cases of failure of one or two QH circuits (each including two QH strips) are analysed; the less likely case of complete failure of a CLIQ unit corresponds to the case O-QH only. Note that the case of double QH failure includes the case of one single failure occurring in a magnet with one QH circuit permanently damaged.

Figures 6a 6f and Table 11 show the simulated T_{hot}, $U_{g,peak}$ and $U_{t,peak}$ in the considered failure scenarios after a quench at I_{nom} and I_{ult}. Uncertainty ranges are due to the different locations of the initial quench and of the failing QH strips.

With the O-QH configuration, at nominal current one QH failure would result in an increase of Thot close to or above the 350 K target; and two QH failures close to the 385 K hard limit. At ultimate current, one failure would be sufficient to reach the 385 K hard limit. On the contrary, even considering two QH failures the protection options including I QH or CLIQ yield a Thot increase with respect to the no failure case of only 30 and 5 K, respectively, both at I_{nom} and I_{ult}.

The peak turn to turn voltage increases by about 15% for double failures in an O QH system, and is virtually unaffected if I QH or CLIQ are installed.

Note that a worst case analysis including a combination of failure cases and non uniform strand parameters would yield even higher T_{hot}, $U_{g,peak}$ and $U_{t,peak}$.

Additional failure cases are under study but are not included in this document, including:

- One capacitor of one CLIQ unit going in open circuit
- One capacitor of one CLIQ unit going in short circuit
- Fuse of one of the QH power supply unit blowing up
- One parallel diode not conducting

Table 11. Failure case analysis. Simulated hot-spot temperature, peak voltage to ground and peak turn to turn voltage obtained for one failure or two simultaneous failures of QH circuits, at nominal and at ultimate current. Uncertainty ranges are due to the different locations of the initial quench and of the failing QH circuits

Configuration	T_{hot} [K]			$U_{g,peak}$ [V]			$U_{t,peak}$ [V]		
	No f	1	2	No f	1	2	No f	1	2
Nominal current									
O-QH	330-345	345-362	363-384	577	702	868	113	122	132
O-QH + I-QH	251-253	255-266	277-283	561	716	928	83	90	100
O-QH + CLIQ	236-237	238-240	239-242	641	668	666	83	84	86
Ultimate current									
O-QH	352-369	364-385	379-406	808	916	1068	133	141	152
O-QH + I-QH	276-279	279-292	301-310	725	898	1128	101	109	120
O-QH + CLIQ	260-262	261-264	262-267	874	910	909	101	103	105

8 FUTURE STEPS

In several simulated discharges, relatively high voltages to ground were simulated, in particular in the configuration including O QH and CLIQ at ultimate current. The parameters of the CLIQ unit, namely the charging voltage and capacitance of the capacitor bank and the resistance of its discharge circuit, can be optimized in order to try and reduce the peak voltages to ground while still assuring good protection performance in terms of hot spot temperature. After CLIQ experimental results from the first MQXFS1b model magnet are available, a review of CLIQ baseline parameters is advised.

All simulations presented in this document assume QH delays calculated using default QH parameters. In the case of QH attached to the inner layer of the coils, these delays are shorter than those experimentally observed in the first MQXFS1a model magnet. However, it is expected that the performance of I QH protecting future MQXF magnets will improve and match the simulated performance.

A spread in the QH delays achieved by different strips attached to the same magnet may cause an unbalance temperature and voltage distribution, which needs to be evaluated. Furthermore, the effect on the quench protection performance of a degradation of components over the life of the machine is to be carefully considered.

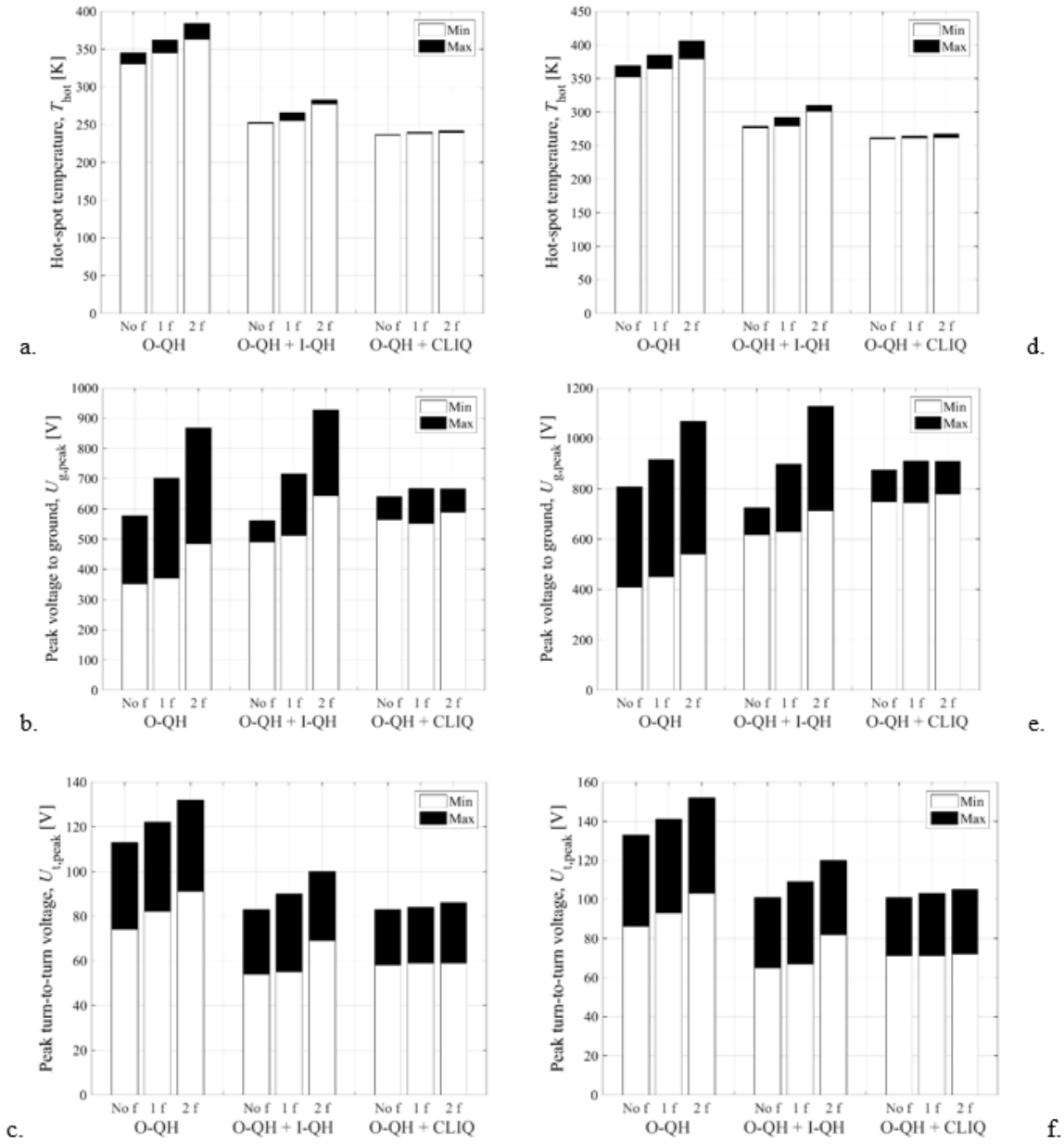

Figure 6. Failure case analysis. Simulated hot spot temperature (a, d), peak voltage to ground (b, e) and peak turn to turn voltage (c, f) obtained for one failure ("1f") or two simultaneous failures ("2f") of QH circuits. Uncertainty ranges are due to the different locations of the initial quench and of the failing QH circuits. a-b-c. At nominal current. d-e-f. At ultimate current.

9 REFERENCE WORST-CASE PEAK VOLTAGES TO GROUND

This section summarizes the reference worst-case peak voltages to ground $U_{g,ref}$, which will be used to define the test voltages during the electrical quality assurance process. A safety factor will be applied to such value to account for model and material property inaccuracies and to have margin in the case of unexpected failures. The test voltage will be $U_{g,test}=2U_{g,ref}+500$ V. The same test voltage will be applied to magnets manufactured by CERN and LARP.

The guidelines followed to define the reference worst-case peak voltages to ground are:

- The values at nominal current (not at ultimate current) are chosen as a reference; the safety margin will cover the case at ultimate current.
- The worst-case failure includes 2 QH circuit failing simultaneously.

- The influence of strand parameters was studied, but corrective measures can be taken to avoid reaching the worst conditions. Hence, the reference values will not consider the influence of strand parameters.

Following these guidelines, the voltage to ground reference values will be those reported in columns "2" of Table 11 of this report: 868, 928, 667 V to ground for the O-QH, O-QH+I-QH, O-QH+CLIQ cases, respectively.

Before the publication of this report, the suggested reference value was 520 V, calculated in the case of O-QH+CLIQ [10]. The increase with respect to this value comes from the improvement in the model accuracy and from the detailed analysis of the effect of the initial hot-spot position.

However, it is recommended that no correction of the test values during electrical electrical quality be asked, considering that prudent safety margins were applied.

10 ANALYSIS OF THE PEAK CURRENTS THROUGH CROWBARS OF TRIM POWER SUPPLIES AND CURRENT LEADS

The peak currents and thermal loads occurring in each element of the electrical circuit are an important piece of information for their thermo-electrical design. In Section 5.1, two examples of circuit discharges after quench were given. In this section, a very conservative scenario is considered in order to calculate the worst-case values. It is assumed that one entire coil (four poles) quenches instantaneously at nominal current, and the quench protection system is activated 16 ms later (5 ms for quench detection, 10 ms validation time, 1 ms triggering time). The faster discharge of the current of the first magnet to quench causes relatively large currents to flow through the current leads, the crowbar of the main and trim power supplies, and the circuit parallel elements. In order to determine the worst-case scenario, various simulations are performed assuming different initial currents in the trim power supplies, and different positions of the first magnet to quench.

Table 12 summarizes the highest peak currents and thermal loads calculated with this analysis, for the O-QH and O-QH+CLIQ protection configurations. Note that in the case O-QH+I-QH the peak currents and thermal loads are very similar to O-QH+CLIQ, whereas the peak current changes are very similar to O-QH. For the O-QH+CLIQ case, peak currents up to 4.4 kA can flow through Leads B and D and through the crowbars of TS1 and TS3, which are dimensioned for carrying a DC current of 2 kA during normal operation; and peak currents up to 3.2 kA can flow through Lead C and through the crowbar of TS2, which are dimensioned for carrying a DC current of 120 A during normal operation. The thermal loads deposited in the 2 kA and 120 A elements are 2.3 and 1.0 MIIt, respectively.

Foir the O-QH case, both peak currents and thermal load increase.

Table 12. Simulated worst-case peak currents (Ip), thermal loads (TL) and current changes (dI/dt) in various circuit elements, after an instantaneous quench of the entire Q2b coil at nominal current.

Elements	O-QH			O-QH+CLIQ*		
	Ip [kA]	TL [MIIt]	dI/dt* [kA/s]	Ip [kA]**	TL [MIIt]**	dI/dt [kA/s]
Lead A	16.5	29.8	106	16.5	26.4	170
Lead B	5.6	3.9	53	4.4	2.3	80
Lead C	4.9	2.5	10	3.2	1.0	19
Lead D	5.6	3.9	53	4.4	2.3	80
Lead E	16.5	29.8	106	16.5	26.4	192
Crowbar TS1	5.6	3.9	53	4.4	2.3	80
Crowbar TS2	4.9	2.5	10	3.2	1.0	19

Crowbar TS3	5.6	3.9	53	4.4	2.3	80

*Values in the case O-QH+I-QH that are very similar to O-QH

**Values in the case O-QH+I-QH that are very similar to O-QH+CLIQ

Note: Values of dI/dt are copied from Table 7.

The simulated currents flowing in the various circuit elements in two worst-case scenarios are plotted in Figures 7 and 8:

- Worst-case for Leads B and D, and for the three crowbars of the trim power supplies (see Figure 7). Initial currents: I_{MS}=16.5 kA, I_{TS1}=I_{TS2}=-2 kA, I_{TS3}=-0.12 kA. Quench of the entire Q2b coil (all four poles).
- Worst-case for Lead C (see Figure 8). Initial currents: I_{MS}=16.5 kA, I_{TS1}= I_{TS2}=I_{TS3}=0. Quench of the entire Q2b coil (all four poles).

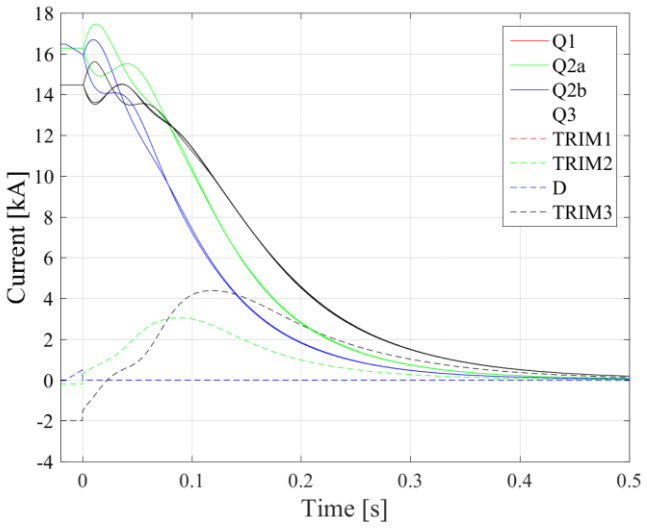

(a)

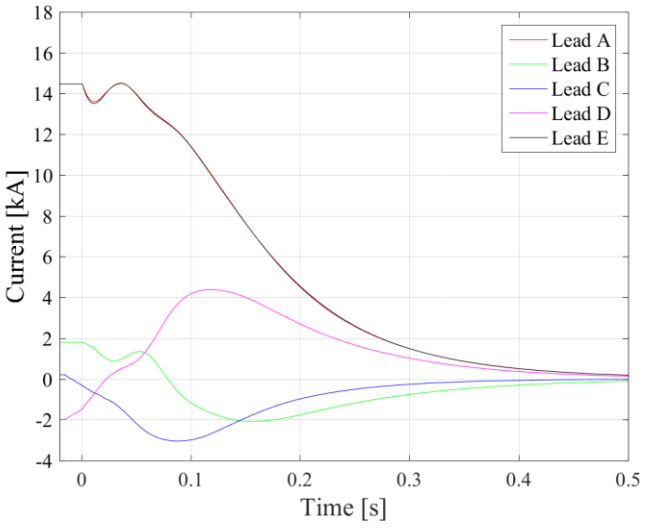

(b)

Figure 7. Simulated currents in the magnets and parallel diodes (a) and in the current leads (b) after an instantaneous quench of the entire Q2b coil at nominal current. Initial current provided by the main and trim power supplies are: I_{MS}=16.5 kA, I_{TS1}=I_{TS3}=-2.0 kA, and I_{TS2}=-0.12 kA.

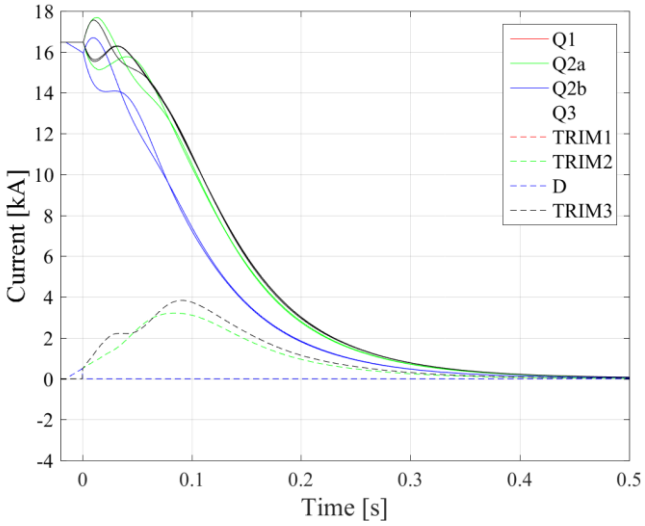

(a)

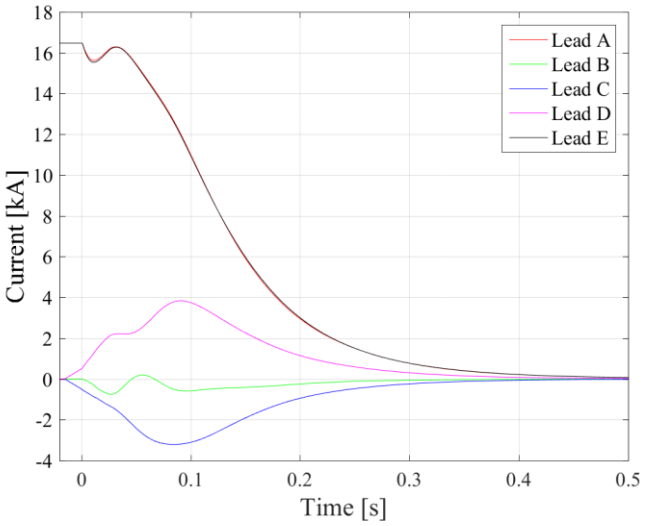

(b)

Figure 8. Simulated currents in the magnets and parallel diodes (a) and in the current leads (b) after an instantaneous quench of the entire Q2b coil at nominal current. Initial current provided by the main and trim power supplies are: I_{MS}=16.5 kA, I_{TS1}=I_{TS2}=I_{TS3}=0.

11 CONCLUSION

The results of the quench protection studies for the High-Luminosity LHC inner triplet circuit are presented. The studies include a comparison between the performance of different protection system configurations, sensitivity analyses to conductor parameters, and failure scenarios.

The behaviour of the circuit, updated to the current baseline, is simulated and the expected peak currents and current rate changes are summarized.

Three options for the quench protection system are analysed: one including only quench heaters attached to the coil's outer layer; one including quench heaters attached to both coil's layers; and one including outer quench heaters and CLIQ units.

For each considered protection option, the simulated hot spot temperature, peak voltage to ground, and peak turn to turn voltage at nominal and ultimate current are calculated, taking into account the effect of a different position of the initial quench in the coil.

The effect of strand parameters on the quench protection performance is studied in detail and the expected uncertainty ranges are provided.

From the simulation results one can observe that the protection option relying only on outer quench heaters can result in a hot spot temperature close to or higher than the target limit of 350 K already at nominal current, and close to or higher than the hard limit of 385 K at ultimate current.

The peak voltages to ground significantly depend on the initial quench location and on the strand parameters. Several simulations show relatively high peak values, in particular at ultimate current. Solutions including a CLIQ unit result often in higher voltages to ground; a revision of the CLIQ parameters to reduce the voltages to ground is suggested.

One example is presented, which considers the case of a magnet composed of one low RRR pole and three high RRR poles. Peak voltages to ground significantly higher than the cases with uniform strand parameters are simulated. The study shows how the electrical order of the poles can be optimized to reduce this unwanted effect.

This example stresses the importance of monitoring the strand parameters during the manufacturing process and of optimizing the order of the poles based on this information. It is strongly advised that the pole order for each produced magnet is selected based also on quench protection considerations.

Finally, the impact of the failure of one or two QH circuits is assessed. In the case of a protection option including only outer quench heaters, the simulated hot spot temperature are close to or above unacceptable values.

In the cases of outer quench heaters, or combination of inner and outer quench heaters, the peak voltages to ground in QH failure scenarios increase considerably.

Further studies are foreseen to propose optimized values of the quench protection system parameters, revised after the model magnet test campaigns, and to evaluate the impact on the protection performance of a degradation of the system components over the life of the machine.

12 REFERENCES

[1] E. Ravaioli, “CLIQ”, PhD thesis, University of Twente, 2015.

[2] J. P. Burnet, “Power converters: operational aspects”, Conceptual design review of the magnet circuits of the HL LHC, CERN, March 2016.

[3] V. Marinozzi, et al., “Study of Quench Protection for the Nb_3Sn Low Quadrupole for the LHC Luminosity Upgrade (HiLumi-LHC)”, IEEE Trans. Appl. Supercond., vol. 25, no. 3, June 2015, doi: 10.1109/TASC.2014.2383435.

[4] G. Manfreda et al., “Quench Protection Study of the Nb_3Sn Low-β Quadrupole for the LHC Luminosity Upgrade”, IEEE Trans. Appl. Supercond., vol. 24, no. 3, June 2014, doi: 10.1109/TASC.2013.2285099.

[5] E. Ravaioli et al., “Advanced Quench Protection for the Nb_3Sn Quadrupoles for the High Luminosity LHC”, IEEE Transactions on Applied Superconductivity, vol. 26, 2016.

[6] G. Ambrosio, P. Ferracin, et al., “MQXFS1 QUADRUPOLE DESIGN REPORT”, LARP note, 2015.

[7] P. Ferracin et al., “Magnet Design of the 150 mm Aperture Low-β Quadrupoles for the High Luminosity LHC”, IEEE Trans. Appl. Supercond., vol. 24, no. 3, June 2014, doi: 10.1109/TASC.2013.2284970.

[8] M. Maciejewski, E. Ravaioli, B. Auchmann, A.P. Verweij, and A. Bartoszewicz, “Automated Lumped-Element Simulation Framework for Modelling of Transient Effects in Superconducting Magnets”, Proceedings of the 20th International Conference on Methods and Models in Automation and Robotics, 2015.

[9] E. Ravaioli, B. Auchmann, M. Maciejewski, H.H.J. ten Kate, and A.P. Verweij, “Lumped-Element Dynamic Electro-Thermal model of a superconducting magnet”, Cryogenics, 2016.

[10] G. Ambrosio, “Maximum allowable temperature during quench in Nb3Sn accelerator magnets”, CERN Yellow Report CERN-2013-006, pp.43-46, 2013, doi: 10.5170/CERN-2013-006.43.

[10] E. Ravaioli, “The inner triplet circuit”, Conceptual design review of the magnet circuits of the HL LHC, CERN, March 2016.